

Indicator Functions: Distilling the Information from Gaussian Random Fields

Andrew Repp^{1*}, Ravi K. Sheth^{2†}, István Szapudi^{3‡}, and Yan-Chuan Cai^{4§}

¹*Christian Liberty Academy, Kea'au, HI 96749, USA*

²*Department of Physics and Astronomy, University of Pennsylvania, Philadelphia, PA 19104, USA*

³*Institute for Astronomy, University of Hawaii, 2680 Woodlawn Drive, Honolulu, HI 96822, USA*

⁴*Institute for Astronomy, University of Edinburgh, Royal Observatory, Blackford Hill, Edinburgh, EH9 3HJ, UK*

10 June 2025; submitted to MNRAS

ABSTRACT

A random Gaussian density field contains a fixed amount of Fisher information on the amplitude of its power spectrum. For a given smoothing scale, however, that information is not evenly distributed throughout the smoothed field. We investigate which parts of the field contain the most information by smoothing and splitting the field into different levels of density (using the formalism of indicator functions), deriving analytic expressions for the information content of each density bin in the joint-probability distribution (given a distance separation). We find that the information peaks at moderately rare densities (where the number of smoothed survey cells $N \sim 100$). Counter-intuitively, we find that, for a finite survey volume, indicator function analysis can outperform conventional two-point statistics while using only a fraction of the total survey cells, and we explain why. In light of recent developments in marked statistics (such as the indicator power spectrum and density-split clustering), this result elucidates how to optimize sampling for effective extraction of cosmological information.

Key words: cosmology: theory – cosmology: miscellaneous – methods: statistical

1 INTRODUCTION

The Λ CDM framework neatly explains the bulk of available cosmological data (e.g., [Planck Collaboration et al. 2020](#)), and a major goal of current and future surveys is to measure these parameters more precisely. Such surveys include CMB-mapping efforts like CMB-S4 ([Abazajian et al. 2019](#)); line intensity surveys like CHIME (Canadian Hydrogen Intensity Mapping Experiment, [Newburgh et al. 2014](#)) and COMAP (CO Mapping Array Project, [Kovetz et al. 2017](#)); and galaxy surveys like DESI (Dark Energy Spectroscopic Instrument, [DESI Collaboration et al. 2016](#)), *Euclid* ([Laureijs et al. 2011](#)) and *Roman* ([Akeson et al. 2019](#)).

Fisher information provides a useful metric for the constraining power of these surveys. Unfortunately, more data does not necessarily translate into more information. In particular, the standard analysis tools (i.e., power spectrum and correlation function) exhibit an information plateau at higher wavenumbers ([Neyrinck and Szapudi 2007](#); [Lee and Pen 2008](#); [Wolk et al. 2015](#)).

Multiple strategies exist for circumventing this plateau. One is to apply Gaussianizing transformations (e.g., the log transform, [Neyrinck et al. 2009](#), given the approximate

lognormality of the matter field). Another strategy is to combine power spectrum analysis with local density information such as counts-in-cells, thus capturing the density-dependence of clustering. This procedure represents a variety of mark-correlation analysis ([Sheth 1998](#); [Beisbart and Kerscher 2000](#); [Szapudi et al. 2000](#); [Skibba et al. 2006](#)), with densities serving as marks ([Martino and Sheth 2009](#); [White and Padmanabhan 2009](#); [Chiang et al. 2015](#); [White 2016](#); [Gruen et al. 2016, 2018](#); [Massara et al. 2021](#); [Paillas et al. 2021, 2023](#)); see in particular the pioneering work of [Abbas and Sheth \(2005, 2007\)](#), as well as [Paranjape et al. \(2018\)](#); [Shi and Sheth \(2018\)](#); [Alam et al. \(2019\)](#). In addition, since each density bin defines its own set of regions in a survey volume, the simultaneous use of multiple density bins is a species of multitracer analysis ([McDonald and Seljak 2009](#); [Bernstein and Cai 2011](#); [Hamaus et al. 2011](#); [Barreira and Krause 2023](#); [Nikakhtar et al. 2024](#)).

[Repp and Szapudi \(2022\)](#) introduced indicator functions as a unifying framework for such density-dependent analyses. This framework enables us to understand where the survey's information comes from, facilitating the design of more efficient information-extraction methods. In this work, we apply indicator functions to Gaussian random fields and demonstrate analytically that a large amount of the information typically resides in a small number of density extrema. Given the importance of optimal weighting (e.g., [Cai et al. 2011](#)), it is significant that we can focus our attention on the most information-rich (as opposed to noise-dominated)

* arepp@clahawaii.org

† shethrk@upenn.edu

‡ szapudi@ifa.hawaii.edu

§ cai@roe.ac.uk

survey cells, thus distilling out the bulk of the field’s information. Such information-locative knowledge should increase the efficiency of survey data analysis, as well as assisting formulation of measures which are more robust to various kinds of systematics.

We focus this work on the amplitude of the power spectrum; thus, in this paper, “information” denotes specifically information on this amplitude; however, the analysis should apply to any amplitude-like parameter. It might not apply to shape parameters, since we assume that we already know the shape of the power spectrum.

We organize the paper as follows: in Section 2 we derive an expression for the total amount of information in an n -point Gaussian field. Section 3 defines indicator functions and their correlations. Section 4 then provides analytic expressions for the information in indicator correlations for a Gaussian field. In Section 5 we test the accuracy of our expressions, with discussion and conclusion occupying the final two sections.

2 INFORMATION IN A GAUSSIAN DISTRIBUTION

We start by establishing the total amount of information (on σ^2 , the amplitude of the power spectrum) contained in a Gaussian field.

Consider first a one-point probability distribution function $\mathcal{P}(\delta)$ with zero mean and variance σ^2 . The Fisher information on $\ln \sigma^2$ is

$$I_1 \equiv \int d\delta \mathcal{P}(\delta) \left(\frac{d \ln \mathcal{P}(\delta)}{d \ln \sigma^2} \right)^2 \quad (1)$$

For a Gaussian distribution,

$$\mathcal{P}(\delta) = \frac{\exp(-\delta^2/2\sigma^2)}{\sqrt{2\pi\sigma^2}}. \quad (2)$$

Thus, if we define $\nu \equiv \delta/\sigma$, the information $I_1 = \langle (\nu^2 - 1)^2/2^2 \rangle = 1/2$.

Now consider the two-point distribution

$$\mathcal{P}_2(\delta_1, \delta_2) = \mathcal{P}(\delta_1) \mathcal{P}(\delta_2|\delta_1), \quad (3)$$

and suppose that both one point distributions $\mathcal{P}(\delta_1)$ and $\mathcal{P}(\delta_2)$ have mean zero and variance σ^2 . The Fisher information on $\ln \sigma^2$ is now

$$\begin{aligned} I_2 &\equiv \int d\delta_1 d\delta_2 \mathcal{P}(\delta_1, \delta_2) \left(\frac{d \ln \mathcal{P}_2}{d \ln \sigma^2} \right)^2 \\ &= \int d\delta_1 \mathcal{P}(\delta_1) \int d\delta_2 \mathcal{P}(\delta_2|\delta_1) \times \\ &\quad \left(\frac{d \ln \mathcal{P}(\delta_1)}{d \ln \sigma^2} + \frac{d \ln \mathcal{P}(\delta_2|\delta_1)}{d \ln \sigma^2} \right)^2 \\ &= I_1 + \int d\delta_1 \mathcal{P}(\delta_1) I_{2|1}. \end{aligned} \quad (4)$$

For a bivariate Gaussian, $\mathcal{P}(\delta_2|\delta_1)$ is also Gaussian, with mean $\mu_{2|1} \equiv \delta_1 \langle \delta_2 \delta_1 \rangle / \sigma^2$ and variance $\sigma^2 (1 - \gamma^2)$, where $\gamma = \langle \delta_2 \delta_1 \rangle / \sigma^2$. The amplitude of the power spectrum cancels out in the ratios defining $\mu_{2|1}$ and γ . So, if we let $\nu_{2|1} = (\nu_2 - \gamma \nu_1) / \sqrt{1 - \gamma^2}$, then $I_{2|1} = \langle (\nu_{2|1}^2 - 1)^2/4 \rangle = 1/2$, making $I_2 = 2I_1$.

By repeating this logic, it is straightforward to see that the information on $\ln \sigma^2$ contained in an n -point Gaussian distribution generalizes to $I_n = nI_1 = n/2$.

We can extend this result to lognormal distributions. If we define $A = \ln(1 + \delta)$ and assume A is Gaussian, then

$$\mathcal{P}(A) = \frac{e^{-(A + \sigma_A^2/2)^2/2\sigma_A^2}}{\sqrt{2\pi\sigma_A^2}}, \quad (5)$$

with $\langle A \rangle = -\sigma_A^2/2$. Since $1 + \sigma_\delta^2 = \exp(\sigma_A^2)$, we must decide if we are interested in the amplitude of $P_A(k)$ or of $P_\delta(k)$. The form above suggests that it is more convenient to work with σ_A^2 , since then the Fisher information is

$$I_1 = \langle [\nu_A^2/2 - 1/2 - \sigma_A \nu_A/2]^2 \rangle = (1 + \sigma_A^2/2)/2 \quad (6)$$

where $\nu_A \equiv [A - \langle A \rangle]/\sigma_A = [A + \sigma_A^2/2]/\sigma_A$. We can then calculate the Fisher information on $\ln \sigma_\delta^2$ from that on $\ln \sigma_A^2$, given that they are related by the square of the Jacobian $d \ln \sigma_\delta^2/d \ln \sigma_A^2 = (\sigma_A^2/\sigma_\delta^2)(1 + \sigma_\delta^2)$. Since a lognormal is just a monotonic mapping of a Gaussian, one might have thought that the information in the lognormal is the same as that in the Gaussian. The apparent paradox is resolved by noting that the Gaussian variable which transforms to the lognormal (i.e., A) has non-zero mean, and this mean depends on σ_A^2 . Thus, the lognormal provides information about σ_A^2 both through the mean of A and through its variance. Indeed, the expression above tends to the Gaussian information as σ_A^2 approaches 0, consistent with the fact that the lognormal PDF approaches the (zero-mean) Gaussian in this limit. However, $I_2 = 2I_1$ just as for the Gaussian.

3 INDICATOR FUNCTIONS

Density-split statistics (e.g., the density-split clustering analysis in BOSS CMASS, Paillas et al. 2021, 2023; Cuesta-Lazaro et al. 2024; Morawetz et al. 2025) and DESI (Gruen et al. 2016; Friedrich et al. 2018; Gruen et al. 2018) is well-formulated in terms of indicator functions, which we now define.

Following Repp and Szapudi (2022), we say that any bin of values B defines a corresponding *indicator function* on a random field X , so that at every point $x \in X$, the indicator function is unity if and only if $x \in B$. Thus, $I_B : X \rightarrow \{0, 1\}$, such that

$$\mathcal{I}_B(x) = \begin{cases} 1 & x \in B \\ 0 & \text{otherwise.} \end{cases} \quad (7)$$

For X we use the density contrast field $\delta(\mathbf{r}) = \rho(\mathbf{r})/\bar{\rho} - 1$, with ρ being the density at \mathbf{r} . Then for any density bin B , the indicator function \mathcal{I}_B has a value of 1 wherever $\delta \in B$, but vanishes at all other points. Clearly the expected value of the indicator function equals the probability of the bin $\bar{\mathcal{I}}_B = \mathcal{P}(B)$.

We can further normalize the indicator function ($\delta_{\mathcal{I}_B} = \mathcal{I}/\bar{\mathcal{I}}_B - 1$) and define indicator function correlations¹ just as we do with the full random field: given a distance r ,

$$\xi_{I_B}(r) \equiv \frac{\langle \delta_{\mathcal{I}_B}(\mathbf{x}_1) \delta_{\mathcal{I}_B}(\mathbf{x}_2) \rangle_{|\mathbf{x}_2 - \mathbf{x}_1| = r}}{\mathcal{P}(B)^2} - 1 \quad (8)$$

$$= \frac{\mathcal{P}_{11}(B)}{\mathcal{P}(B)^2} - 1, \quad (9)$$

¹ Closely related to the sliced correlations of Neyrinck et al. (2018).

where $\mathcal{P}_{11}(B)$ is the probability that two points separated by a distance of r both fall into density bin B .

In the case of a Gaussian field with weak correlations (so that $\gamma \equiv \xi(r)/\sigma^2 \ll 1$), [Repp and Szapudi \(2022\)](#) derive the following relationship between the standard two-point correlation function $\xi(r)$ and an indicator correlation function $\xi_{IB}(r)$:

$$\xi_{IB}(r) = \frac{\xi(r)\langle\nu\rangle_B^2}{\sigma^2}, \quad (10)$$

where $\nu \equiv \delta/\sigma$, and the average is taken over all cells in bin B . For the remainder of this paper, we suppress notation of the bin B and write ξ_I , understanding that I requires a specified bin.

4 INFORMATION IN INDICATOR CORRELATION FUNCTIONS

Now suppose we have a Gaussian random field which evolves in a linear manner. Let A_z represent the amplitude of the power spectrum $P(k)$ with respect to some fiducial value (i.e., the primordial amplitude A_s after being evolved to reference time z). If $P_{\text{fid}}(k)$ is the fiducial power spectrum value, then

$$A_z \equiv \frac{P(k)}{P_{\text{fid}}(k)} = \frac{\xi(r)}{\xi_{\text{fid}}(r)}, \quad (11)$$

where $\xi(r)$ and $\xi_{\text{fid}}(r)$ are the two-point correlation function and its fiducial value at distance r . Writing $\xi(r) = \gamma(r)\sigma^2$, we can say

$$A_z = \frac{\sigma^2}{\sigma_{\text{fid}}^2}. \quad (12)$$

We want to calculate the information on A_z contained in the indicator-function correlations $\xi_I(r)$, within a given interval of r -values.

The indicator correlation function itself is thus our observable. It has a theoretical value (the average value over an ensemble of surveys) for which we reserve the notation $\xi_I(r)$. The actual observed values of the indicator-function correlations will differ stochastically from survey to survey; we denote the observed value as $\hat{\xi}_I(r)$.

Determining the information in $\xi_I(r)$ requires calculation of the expected value of $((\partial/\partial A_z)\ln\hat{\xi}_I(r))^2$, which in turn requires calculation of the probability distribution of $\hat{\xi}_I(r)$. Thus, given a theoretical $\xi_I(r)$, we must determine the likelihood of observing a given $\hat{\xi}_I(r)$.

4.1 Probability Distribution for $\hat{\xi}_I(r)$

Suppose we have a survey consisting of N_c cells (i.e., smoothed with a top-hat filter at discrete points); we choose a bin B of densities to determine our indicator function. We also choose a bin R of r -values for our correlation function.

Let \hat{N}_1 be the number of the cells on which the indicator function is unity (i.e., the number in density bin B). Let N_p be the number of *pairs* of cells (of any density) separated by a distance $r \in R$. Let \hat{N}_{11} be the number of such pairs on which the indicator function for *both* cells is unity.

Say the probability of a cell falling into density bin B is P_1 , and the probability of a pair of cells (separated by distance

$r \in R$) both falling into B is P_{11} . Then the expected value of the (normalized) indicator-function correlation is

$$\xi_I(r) = \frac{P_{11}}{P_1^2} - 1. \quad (13)$$

However, the observed correlation is

$$\hat{\xi}_I(r) = \frac{\hat{P}_{11}}{\hat{P}_1^2} - 1, \quad (14)$$

where \hat{P}_1 and \hat{P}_{11} are the empirical probabilities \hat{N}_1/N_c and \hat{N}_{11}/N_p , respectively. We want to determine the likelihood $\mathcal{P}(\hat{\xi}_I(r))$ given underlying probabilities P_1 out of N_c cells, and given P_{11} out of N_p pairs, and we obtain this likelihood by differentiating the cumulative distribution function:

$$\mathcal{P}(\hat{\xi}_I) = \frac{d}{d\hat{\xi}_I} \Pr(\hat{\xi}_I \leq \hat{\xi}_I) \quad (15)$$

$$= \frac{d}{d\hat{\xi}_I} \int d\hat{P}_1 \int_0^{\hat{P}_1^2(1+\hat{\xi}_I)} d\hat{P}_{11} \Pr(\hat{P}_{11}|\hat{P}_1) \Pr(\hat{P}_1) \quad (16)$$

$$= \int d\hat{P}_1 \hat{P}_1^2 \Pr(\hat{P}_{11} = \hat{P}_1^2(1+\hat{\xi}_I)|\hat{P}_1) \Pr(\hat{P}_1). \quad (17)$$

To obtain an expression for this integral,² let us assume that the empirical probabilities \hat{P}_1 scatter about the expected value P_1 with variance σ_1^2 , so that

$$\Pr(\hat{P}_1 = x) = G(x; P_1, \sigma_1^2); \quad (18)$$

likewise, we assume a Gaussian distribution for the conditional probability in Equation 17:

$$\Pr(\hat{P}_{11} = y | \hat{P}_1 = x) = G(y; x^2(1+\xi_I), \sigma_{1|1}^2). \quad (19)$$

Thus we obtain the following distribution for $\mathcal{P}(\hat{\xi}_I(r))$:

$$\mathcal{P}(\hat{\xi}_I) = \frac{1}{2\pi\sigma_{1|1}\sigma_1} \times \int dx x^2 \exp\left(-\frac{x^4(\hat{\xi}_I - \xi_I)^2\sigma_1^2 + (x - P_1)^2\sigma_{1|1}^2}{2\sigma_{1|1}^2\sigma_1^2}\right). \quad (20)$$

Performing this integration is nontrivial. Let us assume that $\sigma_1 \ll P_1$. Using the expression from [Repp and Szapudi \(2021\)](#), one can show that this assumption is equivalent to

$$N_1 \gg \frac{1}{1 - \xi_I} \approx 1. \quad (21)$$

So as long as a decent number of survey cells occupy the density bin under consideration, this assumption should be valid.

Under this assumption, the exponential is insignificant unless $x \approx P_1$. In this regime,

$$\mathcal{P}(\hat{\xi}_I) \approx \frac{1}{2\pi\sigma_{1|1}\sigma_1} \int dx P_1^2 \exp\left(-\frac{P_1^4(\hat{\xi}_I - \xi_I)^2}{2\sigma_{1|1}^2}\right) \times \exp\left(\frac{-(x - P_1)^2}{2\sigma_1^2}\right) \quad (22)$$

² We cannot assume a binomial distribution since the N_c cells are correlated.

so that

$$\mathcal{P}(\hat{\xi}_I) \approx \frac{P_1^2}{\sigma_{1|1}\sqrt{2\pi}} \exp\left(-\frac{P_1^4(\hat{\xi}_I - \xi_I)^2}{2\sigma_{1|1}^2}\right). \quad (23)$$

Thus, in this regime, the measured values of the indicator function correlations will be normally distributed with mean ξ_I and variance $\sigma_{1|1}^2/P_1^4$.

We must now estimate $\sigma_{1|1}^2$, the variance of the (conditional) two-point probability measurement \hat{P}_{11} in Equation 19. We do so as follows.

In any realization of this field, the number of cells in density bin B is $\hat{N}_1 = N_c \hat{P}_1$. Suppose that for any cell x_0 in the survey, there are $2k$ other cells a distance $r \in R$ from x_0 .³ Then the total number of pairs of cells separated by $r \in R$ is $N_p = N_c k$ (dividing by 2 to avoid double-counting the pairs).

Now, we know there are $\hat{N}_1 k$ cells in density bin B . If we focus on the $2\hat{N}_1 k$ cells the requisite distance away from them, those cells will also be in B with probability $P_1(1+\xi_I)$. Therefore, the total number of pairs of cells (separated by $r \in R$) for which the indicator function on both is unity is given by the binomial distribution:

$$\hat{N}_{11} \sim \text{Bin}(\hat{N}_1 k, P_1(1+\xi_I)). \quad (24)$$

Thus we have the conditional variance of $\hat{P}_{11} = \hat{N}_{11}/N_p$:

$$\text{Var}(\hat{P}_{11}|\hat{P}_1) = \frac{1}{N_p^2} \text{Var}(\hat{N}_{11}|\hat{N}_1) \quad (25)$$

$$= \frac{1}{N_p} \hat{P}_1 P_1(1+\xi_I)(1-P_1(1+\xi_I)). \quad (26)$$

Therefore the expected value of this conditional variance (averaging across empirical probabilities \hat{P}_1) is

$$\sigma_{1|1}^2 = \langle \text{Var}(\hat{P}_{11}|\hat{P}_1) \rangle = \frac{P_1^2}{N_p} (1+\xi_I)(1-P_1(1+\xi_I)). \quad (27)$$

We note that Equation 27 is still an approximation, since if two cells x_1 and x_2 are both a distance r from cell x_0 , the values of x_1 and x_2 are correlated, and strictly speaking the binomial distribution does not apply. In particular, there is a dependence on the value of k , such that as k increases, the variance $\sigma_{1|1}^2$ will in fact exceed the value given in Equation 27.

However, if we assume this expression for $\sigma_{1|1}^2$, we can from Equation 23 conclude that the variance of $\hat{\xi}_I$ is

$$\sigma_{\hat{\xi}_I}^2 = \frac{(1+\xi_I)(1-P_1(1+\xi_I))}{P_1^2 N_p}, \quad (28)$$

and if we work to first order in ξ_I , we can write

$$\sigma_{\hat{\xi}_I}^2 = \frac{1-P_1+\xi_I(1-2P_1)}{P_1^2 N_p}, \quad (29)$$

For the expected value of the distribution, $\langle \hat{\xi}_I \rangle$ is simply the indicator correlation ξ_I . Using the expression in [Repp and Szapudi \(2022\)](#) (for Gaussian fields in the linear regime), we can write

$$\langle \hat{\xi}_I \rangle = \frac{\xi \delta^2}{\sigma^4} = \frac{\gamma \delta^2}{A_z \sigma_{\text{fid}}^4}. \quad (30)$$

We note again that $\gamma \equiv \xi/\sigma^2$, and that ξ_I denotes the indicator correlation, while ξ denotes the standard two-point correlation of the field δ .

³ This assumes periodic boundary conditions; otherwise it is a good approximation if r is small compared to the survey size.

4.2 Calculating Fisher Information

Given this PDF for $\hat{\xi}_I$, we can now calculate the Fisher information on the amplitude A_z contained in the observable $\hat{\xi}_I$, given a distance range R . We assume a Gaussian distribution for δ , so that $P_1 = G(\delta; 0, \sigma^2)$.⁴

Writing Δ for $\hat{\xi}_I - \xi_I$, and writing V for $\sigma_{\hat{\xi}_I}^2 = \langle \Delta^2 \rangle$, we have

$$\mathcal{P}(\hat{\xi}_I) = \frac{1}{\sqrt{2\pi V}} \exp\left(-\frac{\Delta^2}{2V}\right). \quad (31)$$

Then the information on A_z is

$$\mathcal{I}_{\sigma^2} = \left\langle \left(\frac{d}{dA_z} \ln \mathcal{P}(\hat{\xi}_I) \right)^2 \right\rangle \quad (32)$$

$$= \frac{(V')^2}{4V^2} + \langle \Delta^2 \rangle \left(\frac{(\Delta')^2}{V^2} - \frac{(V')^2}{2V^3} \right) + \langle \Delta^4 \rangle \frac{(V')^2}{4V^4} \quad (33)$$

+ $\langle \text{odd powers of } \Delta \rangle$

$$= \frac{1}{2} \left(\frac{V'}{V} \right)^2 + \frac{(\Delta')^2}{V}, \quad (34)$$

where primes denote derivatives with respect to A_z , and the odd moments vanish because of the normal distribution of $\hat{\xi}_I$. From Equation 30 we can write $\Delta' = \gamma \nu^2 / A_z =$ (where again $\nu = \delta/\sigma$) and write the logarithmic derivative $L = (d/dA_z)(\ln V)$ to obtain

$$\mathcal{I}_{A_z} = \frac{L^2}{2} + \frac{\gamma^2 \nu^4}{A_z^2 V}. \quad (35)$$

In this expression, the first term comes from the dependence of V (i.e., $\sigma_{\hat{\xi}_I}^2$) on A_z (via P_1 and ξ_I) in Equation 29; the second comes from the dependence of ξ_I on A_z via Equation 30.

To calculate the first term, we must differentiate Equation 29. Let $\langle \delta \rangle_B$ be the mean density in our bin B , which has width $\Delta\delta$. Then if $\Delta\delta$ is reasonably small, and writing δ for $\langle \delta \rangle_B$, we can approximate

$$P_1 = \frac{1}{\sqrt{2\pi A_z \sigma_{\text{fid}}^2}} \exp\left(\frac{-\delta^2}{2A_z \sigma_{\text{fid}}^2}\right) \Delta\delta, \quad (36)$$

and thus

$$\frac{d}{dA_z} P_1 = \frac{P_1}{2A_z} (\nu^2 - 1). \quad (37)$$

We already have $(d/dA_z)\xi_I = -\xi_I/A_z$. Thus we derive, to first order in γ ,

$$\frac{L^2}{2} = \frac{1}{8A_z^2(1-P_1)^2} \left\{ (P_1-2)^2(\nu^2-1)^2 - \frac{2\gamma\nu^2(\nu^2-1)(P_1-2)(4P_1^2+P_1(\nu^2-7)+2)}{(1-P_1)} \right\} \quad (38)$$

Turning to the second term of Equation 35, we note that it is second-order in γ , and we therefore ignore it.⁵ We thus

⁴ In the linear regime for the cosmological matter distribution, $A_z \propto \sigma^2 = \sigma_{\text{lin}}^2$; on smaller scales, one could adapt these results to the roughly-Gaussian log distribution of $A = \ln(1+\delta)$.

⁵ It is worth noticing however that this term is proportional to N_p , which will be extremely large. Thus its lack—and that of other second-order terms—will have a visible impact in Fig. 1.

obtain the following expression for the information on A_z contained in one indicator function correlation:

$$\mathcal{I}_{A_z} = \frac{1}{A_z^2(1-P_1)} \left\{ \frac{(P_1-2)^2(\nu^2-1)^2}{8(1-P_1)} - \frac{\gamma\nu^2(\nu^2-1)(P_1-2)(4P_1^2+P_1(\nu^2-7)+2)}{4(1-P_1)^2} \right\}. \quad (39)$$

In practice, the second term of this expression is almost negligible, so we can write

$$\mathcal{I}_{A_z} = \frac{1}{A_z^2(1-P_1)} \frac{(P_1-2)^2(\nu^2-1)^2}{8(1-P_1)} \quad (40)$$

This expression is, counterintuitively, *not* proportional to the volume, and we defer discussion of this fact to Section 6. Before presenting our tests of this result, it is thus worthwhile to note the following caveats: Equation 40 assumes (1) that a large number of survey cells fall into the bin (Equation 21); (2) that Equation 27 is a good approximation for the conditional variance; and (3) that the bin width $\Delta\delta$ is reasonably small (see Equation 36).

4.3 The Low-Probability Limit

Whereas Equation 40 assumes the indicator function is unity on a significant number of survey cells ($N_1 \gg 1$), we can also write an expression for the information in the opposite limit ($N_1 \ll 1$), as follows.

Let us assume that $\mathcal{P}(\hat{N}_1 > 1)$ is small enough to ignore, so that $\hat{N}_1 \in \{0, 1\}$. In such a case, we can treat \hat{N}_1 as a Poisson variable with expected value $N_c P_1$, so that $\mathcal{P}(\hat{N}_1 = 1) = N_c P_1$ and $\mathcal{P}(\hat{N}_1 = 0) = 1 - N_c P_1$. In this case there can be no pairs of cells in the density bin, so that $\hat{N}_{11} = 0$ with probability one.

There are thus two possibilities for the $\hat{\xi}_I \equiv \hat{P}_{11}/\hat{P}_1^2 - 1$. If $\hat{N}_1 = 1$, then $\hat{\xi}_I = -1$, which occurs with probability $N_c P_1$; otherwise then $\hat{\xi}_I$ is undefined, with probability $1 - N_c P_1$.

Since we assume the underlying density field is Gaussian, $(d/d\sigma^2)P_1 = (P_1/2\sigma^2)(\nu^2 - 1)$. Summing over the two possibilities for $\hat{\xi}_I$, we obtain for the information (to first order in N_1)

$$\mathcal{I}_{A_z} = \frac{N_1(\nu^2-1)^2}{4A_z^2}. \quad (41)$$

Since this approximation assumes $P_1 N_c \ll 1$, its validity is limited to

$$\frac{\nu^2}{2} \gg \ln \Delta\nu N_c - \ln \sqrt{2\pi} \approx \ln \Delta\nu N_c - 1. \quad (42)$$

5 TESTING THE RESULT

We can now test Equations 40 and 41 in two ways—first, by directly estimating the information from multiple realizations of a Gaussian field; second, by using measurements of an indicator correlation function to constrain the power spectrum amplitude.

5.1 Measurements from Simulations

For our first set of tests of Equation 39, we measure the PDF of $\hat{\xi}_I$ from multiple realizations of a random Gaussian field,

generated⁶ from scalings of the Millennium Simulation linear power spectrum.

We first generate such random fields at 32^3 grid points in a cubical volume (with periodic boundary conditions) of side length $500h^{-1}\text{Mpc}$, simulating a survey with resolution of $\sim 16h^{-1}\text{Mpc}$. Since our goal is to measure the effect of amplitude on $\mathcal{P}(\hat{\xi}_I)$, we use the variance as a proxy for amplitude (i.e., setting $\sigma_{\text{fid}}^2 = 1$ in Equation 12), performing 10,000 realizations with $\sigma^2 = 0.60$ and another 10,000 with $\sigma^2 = 0.65$. (These values approximate $\sigma_8 = 0.8$.) From these we can numerically estimate $(d/d\sigma^2)\mathcal{P}(\hat{\xi}_I)$ for various density bins (ranging from $\delta = -5.5$ to 5.5)⁷ and thus the information in ξ_I for each of these bins. To estimate error bars for our information calculations, we perform 50 sets of such realizations (each set consisting of 10,000 realizations at each of the two values of σ^2).

In the same way, we also generate random fields at 64^3 grid points in a cubical volume of side length $1000h^{-1}\text{Mpc}$, (using the same values for σ^2), thus simulating a survey of eight times the volume.

In both cases, we determine $\hat{\xi}_I(r)$ where r is in the radial distance bin $R = [60, 80)h^{-1}\text{Mpc}$, calculating it directly from \hat{P}_{11} and \hat{P}_1 .

We determine the information on the amplitude in two ways. In the regime for which Equation 23 holds (i.e., where Equation 40 is valid), $\mathcal{P}(\hat{\xi}_I)$ is Gaussian, and so we can get a well-behaved $\mathcal{P}(\hat{\xi}_I)$ by empirically measuring the mean and variance of $\hat{\xi}_I(r)$. The values calculated assuming a Gaussian $\mathcal{P}(\hat{\xi}_I)$ appear as purple points in Fig. 1.⁸ We limit the use of this method to δ -values for which (a) less than ten percent of the normal distribution would fall below -1 , and (b) the expected number of cells N_1 is greater than 10 (pursuant to Equation 21). For comparison, the blue curves show the predictions of Equation 39 (solid where, based on the conditions in the previous sentence, the Gaussian approximation for $\mathcal{P}(\hat{\xi}_I)$ is valid, and dashed otherwise).

To test the low-probability expression of Equation 41, we thus need another method for estimating $\mathcal{P}(\hat{\xi}_I)$. We perform this estimate by binning the measured $\hat{\xi}_I(r)$ -values to obtain $\mathcal{P}(\hat{\xi}_I)$, without making any assumptions about the shape of the distribution. (See Appendix A for our binning algorithm, as well as our correction for random fluctuations between sets of realizations.) The information values calculated from binning appear as green points in Fig. 1. For comparison, the orange curves show the predictions of Equation 41 (solid where $\nu^2/2 \geq \ln \Delta\nu N_c - 0.5$, see Equation 42, dashed otherwise). Both figures use empty circles to denote results falling between the limits of the two predictions (i.e., where both curves are dashed).

Inspection of the figures shows that the approximations (such as working only to first order) made in deriving Equations 40 and 41 do have an impact on their accuracy; in particular it is evident that higher-order terms prevent in-

⁶ Using the package `FyeldGenerator`, Cadiou (2022).

⁷ Since we assume δ is a Gaussian random variable, its domain is unbounded. In cosmological applications δ is non-Gaussian, so that $\delta < -1$ is unphysical. In such cases we could perform the analysis with $A = \ln(1 + \delta)$, which has no lower bound.

⁸ We also correct for the fact that the Gaussian is truncated at $\hat{\xi}_I = -1$. This correction is typically minimal, due to the limits explained in the next sentence.

formation from vanishing at $\nu = \pm 1$, as Equation 40 would indicate. Nevertheless, it is clear that the greatest amount of information comes from ν -values at or near the limit of the Gaussian approximation; in both tested cases, this corresponds to $N_1 \sim 100$ survey cells falling into the density bin. At such densities, the cells are rare enough to be sensitive to changes in amplitude, but not so rare as to be dominated by Poisson noise.

The figure also shows the information contained in the full correlation function $\xi(r)$, obtained by modeling the observed distribution of $\hat{\xi}(r)$ as a Gaussian. Two facts are evident: (a) near the limits of the Gaussian approximation (again, near $N_1 \sim 100$), the indicator correlation function $\xi_I(r)$ contains *more* information than the full correlation function $\xi(r)$; (b) the information in $\xi(r)$ does increase with volume (as expected),⁹ whereas, to first order, the information in $\xi_I(r)$ does not. Nevertheless, the larger volume allows Equation 40 to be valid for larger values of $|\nu|$; thus the information in $\xi_I(r)$ for these liminal ν -values continues to outstrip the information in $\xi(r)$. We discuss both of these counter-intuitive observations below in Section 6.

5.2 Amplitude-Constraining Ability

A second way to test our results is to see if indicator function correlations indeed allow us to constrain the amplitude to (at most) the inverse square root of the information. We can do the same with the full correlation function $\xi(r)$ in order to compare the information in each statistic. We perform this test with the 64^3 -cell realizations from the previous section.

Constraining the amplitude from the measured correlation function is straightforward: since we are assuming that we know γ , we obtain as the amplitude $\sigma_{\text{deduced}}^2 = \hat{\xi}(r)/\gamma$. Each realization thus yields its own deduced amplitude, and the orange histograms in Fig. 2 show the distribution of these values (with their mean and the 1- σ confidence interval).

Constraining the amplitude from the measured indicator correlation function $\hat{\xi}_I(r)$ requires more work. In Equation 30, we could substitute the measured value of $\hat{\xi}_I$ for its expected value and write $\sigma_{\text{deduced}}^2 = \gamma \delta^2 / \hat{\xi}_I$; however, since $\hat{\xi}_I$ scatters around its expected value, it is easy to find realizations in which (say) γ is positive but $\hat{\xi}_I$ approaches zero (blowing the expression up) or, worse yet, is negative (yielding a negative $\sigma_{\text{deduced}}^2$). We shall thus use the measured value of \hat{P}_1 (the number of cells falling into the density bin) to impose a prior on σ^2 . This does not introduce extra information, since we must measure \hat{P}_1 in order to calculate $\hat{\xi}_I$.

In particular, Repp and Szapudi (2021) demonstrate that the variance for a counts-in-cells probability is

$$\sigma_1^2 \equiv \text{Var}(\hat{P}_1) = \frac{P_1(1-P_1)}{N_c} + \frac{N_c-1}{N_c} \bar{\xi}_I^{\neq} P_1^2, \quad (43)$$

where $\bar{\xi}_I^{\neq}$ is the volume-averaged correlation function, excluding same-cell correlations. But by Equation 30,

$$\bar{\xi}_I^{\neq} = \frac{\delta^2}{\sigma^4} \bar{\xi}^{\neq}, \quad (44)$$

⁹ Although it seems not to be completely proportional to volume; comparing the left panel to the right, the volume increases by a factor of 8, whereas the information increases only by 6; recall that in these tests we consider only one bin in r , not the information in the entire correlation function.

and since $\bar{\xi}^{\neq} < \sigma^2$, we conclude that

$$\sigma_1^2 < \frac{P_1(1-P_1)}{N_c} + \frac{\delta^2}{\sigma^2} P_1^2. \quad (45)$$

Since, given a δ -bin, the variance completely determines the theoretical P_1 , we can invert the relationship to write the inferred variance $\hat{\sigma}^2$ as a function of the observed counts-in-cells probability \hat{P}_1 ; thus,

$$\text{Var}(\hat{\sigma}^2) = \text{Var}(\hat{P}_1) \left(\frac{\partial P_1}{\partial \sigma^2} \right)^{-2} \quad (46)$$

$$< \left(\frac{\hat{P}_1(1-\hat{P}_1)}{N_c} + \frac{\delta^2}{\sigma^2} \hat{P}_1^2 \right) \left(\frac{\hat{P}_1}{2\hat{\sigma}^2} \frac{\delta^2 - \hat{\sigma}^2}{\hat{\sigma}^2} \right)^{-2}. \quad (47)$$

Hence, given the observed fraction of counts \hat{P}_1 , we can infer a value for $\hat{\sigma}^2$ and then center the prior distribution (of the actual, underlying amplitude) upon this inferred value:

$$\mathcal{P}(\sigma^2) = \frac{1}{\sqrt{2\pi \text{Var}(\hat{\sigma}^2)}} \exp \left(-\frac{(\hat{\sigma}^2 - \sigma^2)^2}{2\text{Var}(\hat{\sigma}^2)} \right), \quad (48)$$

where we assume equality in Equation 47 as an estimate of $\text{Var}(\hat{\sigma}^2)$.

Furthermore, Equation 29 gives us the expected variance of the measured $\hat{\xi}_I$, allowing us to write

$$\mathcal{P}(\xi_I | \sigma^2) = \frac{1}{2\pi \text{Var}(\hat{\xi}_I)} \exp \left(-\frac{(\xi_I - \hat{\xi}_I)^2}{2\text{Var}(\hat{\xi}_I)} \right). \quad (49)$$

Hence, given a measured value for $\hat{\xi}_I$, we can write

$$\mathcal{P}(\sigma^2 | \hat{\xi}_I) \propto \mathcal{P}(\xi_I | \sigma^2) \mathcal{P}(\sigma^2), \quad (50)$$

from which we can obtain the posterior $\sigma_{\text{deduced}}^2$, as the maximum likelihood value of the amplitude.

Summarizing, in each realization we can measure \hat{P}_1 in the course of measuring $\hat{\xi}_I$. From these measurements, Equations 47–50 let us deduce a posterior value for $\sigma_{\text{deduced}}^2$ from $\hat{\xi}_I$, and the blue histograms in Fig. 2 display these values (along with their mean and 1- σ confidence interval).

When we compare Fig. 2 with the right-hand panel of Fig. 1, we see that our method of constraining σ^2 is not optimally efficient (i.e., it does not necessarily achieve the Cramér-Rao bound). We expect this to be the case for ξ_I because of the approximations we made (e.g., treating Equation 47 as an equality), but it is also the case for ξ : in this case the information is 80, whereas the inverse variance is 62. Nevertheless, this exercise demonstrates that in practice, use of the proper indicator function correlations can deliver tighter constraints on the amplitude than can the correlation function itself.

6 DISCUSSION

We previously noted two counter-intuitive features of Equation 40. The first is that, for sufficiently large $|\nu|$ -values (such that $N_1 \sim 100$), the indicator functions correlations can contain *more* information than the full correlation function. The left-hand panel of Fig. 2 verifies this prediction, showing that indicator function analysis provided tighter constraints on the amplitude than analysis with the full correlation function. This is in part due to the fact that indicator function correlations add counts-in-cells data to the clustering data, so

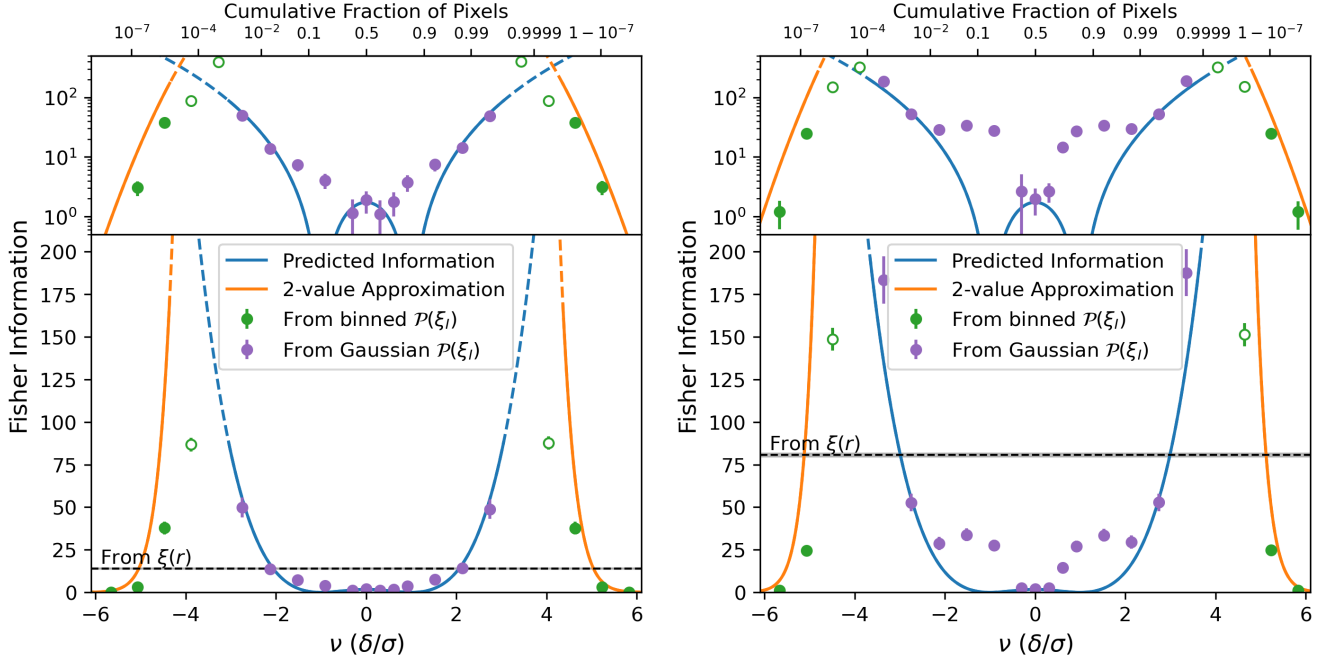


Figure 1. Information on power spectrum amplitude (linear and log scales) from indicator correlation functions $\xi_I(r)$ in the distance bin $r \in [60, 80)h^{-1}\text{Mpc}$, from Gaussian realizations, for various densities $\nu = \delta/\sigma$. The left-hand panel shows results from a cube of $500h^{-1}\text{Mpc}$ per side, divided into 32^3 -cells; the right-hand panel, from a cube of $1000h^{-1}\text{Mpc}$ per side, divided into 64^3 cells. Both panels compare calculated information to the predictions of Equations 39 (blue) and 41 (orange). Dashed portions of the curves indicate values of ν outside the formulas' applicability range. See text for information-calculation methods (yielding green and purple points). Both panels also show the information from the full correlation function $\xi(r)$ for this particular distance bin.

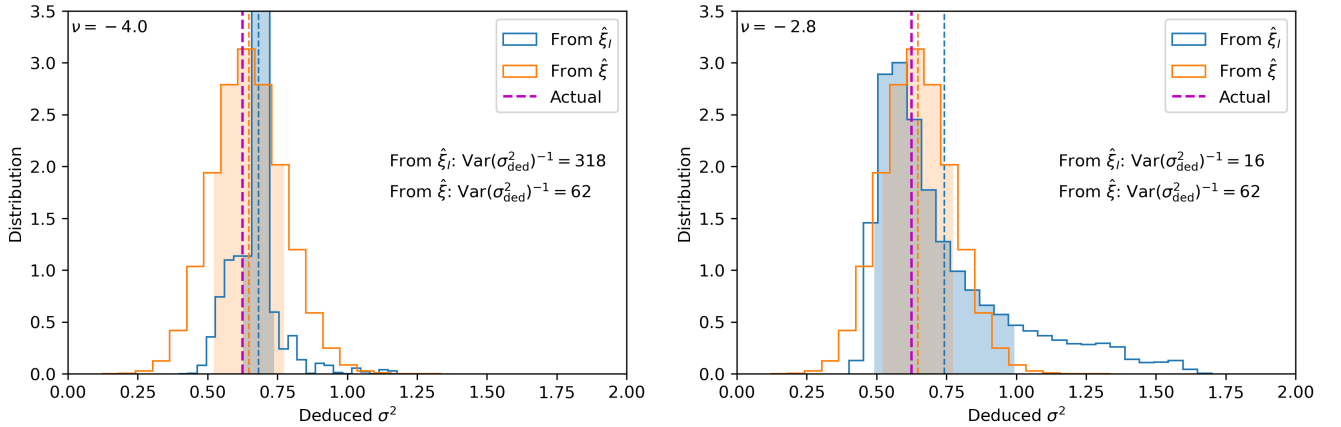


Figure 2. Constraints on the value of σ^2 (proxy for amplitude A_z) deduced from indicator function correlations (ξ_I , blue) and the full correlation function (ξ , orange), in the set of 64^3 -cell realizations described above. Dashed blue and orange lines show mean deduced values, and the shading shows one standard deviation on either side of the mean; the magenta dashed line shows the actual value of ($\sigma^2 = 0.625$) employed to generate the realizations. Left panel: $\nu = \delta/\sigma \approx -4.0$; right panel: $\nu = \delta/\sigma \approx -2.8$. (Since our field is Gaussian, the sign of ν does not matter; cf. Equation 40, which depends on ν^2 only.)

one could expect it to provide more information. However, we must make sense of this feature in light of the fact that two-point correlations indeed capture all the information present in a zero-mean Gaussian field.

It is helpful to remember that in this case we are looking specifically at a particular distance bin R ; to derive the full information we would need to consider all distance bins R (and cross-correlations between them). This is complicated

by the fact that different distance-bins, unlike k -modes, are not independent. Thus, we are not comparing *all* the information inherent in these functions, but only the information at a given separation. What our result shows is, first, that the highest peaks (and lowest valleys) contain the most information, and, second, that ξ averages the different densities in a non-optimal manner, diluting the analysis with non-informative survey cells. The indicator function correlations

distill the information by focusing on the most-informative survey cells (see, e.g., fig. 4 and accompanying discussion in Repp and Szapudi 2022).

The other counter-intuitive feature is the lack of a volume term in Equation 40; comparison of the two panels of Fig. 1 shows that the placement of the blue curve is unchanged under an eight-fold volume increase. To some degree, this is the result of working to first order; the second term of Equation 35 depends on N_p (the number of pairs in the survey volume) but was dropped due to its dependence on γ^2 . Inspection of the figure makes it evident that volume *does* affect the placement of the purple points near $|\nu| = 1$.

However, a much more important reason for the volume-independence is our assumption in Equation 21, which limits the applicability of Equation 40. Even though the placement of the blue curves in Fig. 1 is unaffected by volume, that is not true for the regime of applicability (indicated by the transition from solid to dashed). This dependency reflects the paucity of high peaks in a volume-limited survey; the smaller the survey, the more rare—and thus the less informative—are the high peaks. On the other hand, larger survey volumes allow us to apply Equation 40 to higher values of $|\nu|$. Since N_1 is proportional to survey volume V , the cutoff value of ν^2 depends on $\ln V$. Practically speaking, therefore, the information does depend on volume (albeit indirectly), since volume dictates the applicability of Equation 40.

We can tie these two counter-intuitive features together as follows. By Equation 40, the information scales roughly as ν^4 ; but, when we fix a minimum value for N_1 (say, $N_1 = 100$), Equation 21 produces a maximum value for ν^2 depending on the logarithm of the survey volume. Therefore, the maximum information from $\xi_I(r)$ goes as $(\ln V)^2$. The information in $\xi(r)$, on the other hand, is roughly proportional to V itself. Therefore, for any value of ν , as the survey volume increases, the information in $\xi(r)$ will eventually outstrip the information available in any given $\xi_I(r)$. So in an infinite survey of a Gaussian field, no statistic could outperform $\xi(r)$; for actual surveys, however, $\xi_I(r)$ can often do better.

Our analysis has of course completely ignored the fact that, for realistic matter distributions, the highest peaks are non-linear. One can partially alleviate this non-linearity by performing the analysis on the log density (Neyrinck et al. 2009; Carron and Szapudi 2013; Repp and Szapudi 2017).

In addition, Repp and Szapudi (2022) suggest that indicator functions can selectively excise these nonlinearities, extending linear methods to higher k -values without the complications inherent in perturbation theory. Clipping (Simpson et al. 2011, 2013, 2016) is a conceptually similar method of removing the non-linear peaks (see, e.g., Lombriser et al. 2015; Giblin et al. 2018). Recall that if $I_{p_i}(\mathbf{r})$ is the indicator function field determined by a specific density p_i , then the conventional overdensity $\delta(\mathbf{r})$ is the weighted sum of these indicator functions,

$$\delta(\mathbf{r}) = \sum p_i I_{p_i}(\mathbf{r}), \quad (51)$$

whereas the clipped field is

$$\delta_C(\mathbf{r}) = \sum_{p_i \leq C} p_i I_{p_i}(\mathbf{r}). \quad (52)$$

The results in this work suggest that it might be possible to extract the majority of the information from the highest-density bins ($p_i \approx C$) alone.

Finally, we note the relevance of this analysis to baryon acoustic oscillation (BAO) scales, on which the matter distribution approaches Gaussianity. Our work thus has a straightforward application to measurement of the BAO amplitude. In addition, both Neyrinck et al. (2018) and Xu et al. (2025) show (using sliced correlation functions and density-split statistics, respectively—both closely related to indicator functions) that different density levels yield somewhat different positions for the BAO peak. Since these density-dependent shifts smear out the BAO feature, it follows that analysis at the optimal density levels could provide more accurate measurements of the BAO position, thus sidestepping the model-dependence inherent in most reconstruction methods.

7 CONCLUSION

In summary, when the parameter of interest is the amplitude of the power spectrum, it is straightforward to calculate the total Fisher information contained in an n -point Gaussian field.

However, this information is not evenly distributed among the n cells; rather, certain densities are more information-rich than others. Using indicator functions to select the cells in a given density bin, we can calculate the amount of information (on the power-spectrum amplitude) in the indicator correlation function ξ_I for a given separation distance r . Upon doing so, we find that we obtain the most information by considering cells with high absolute density contrast, as long as the survey contains enough such cells ($N_1 \sim 100$). For typical surveys one can even find density bins for which the indicator correlation function $\xi_I(r)$ contains more information than the full correlation function $\xi(r)$ (at a specified separation distance r), simply because indicator function analysis weights the cells in a more-nearly optimal manner.

Although this work focuses on Gaussian fields (and has not attempted to address discrete sampling), future work will seek to extend these results to more realistic distributions. We conclude that indicator function analysis is a promising strategy for extracting maximal information from cosmological survey data.

DATA AVAILABILITY

The scripts employed in generation and analysis of the Gaussian simulations used in this paper, as well as the data recorded from each simulation, are available upon reasonable request to the authors.

ACKNOWLEDGMENTS

IS acknowledges NASA grants 23-ADAP23-0061 and 24-ADAP24-0074. YC acknowledges the support of the UK Royal Society through a University Research Fellowship. For the purpose of open access, the author has applied a Creative Commons Attribution (CC BY) license to any Author Accepted Manuscript version arising from this submission. This research was supported in part by grant NSF PHY-2309135 to the Kavli Institute for Theoretical Physics (KITP).

REFERENCES

- Abazajian, K., Addison, G., Adshead, P., Ahmed, Z., Allen, S. W., Alonso, D., Alvarez, M., et al.: 2019, *arXiv e-prints* p. arXiv:1907.04473
- Abbas, U. and Sheth, R. K.: 2005, MNRAS **364**(4), 1327
- Abbas, U. and Sheth, R. K.: 2007, MNRAS **378**(2), 641
- Akeson, R., Armus, L., Bachelet, E., Bailey, V., Bartusek, L., Bellini, A., Benford, D., et al.: 2019, *arXiv e-prints* p. arXiv:1902.05569
- Alam, S., Zu, Y., Peacock, J. A., and Mandelbaum, R.: 2019, MNRAS **483**(4), 4501
- Barreira, A. and Krause, E.: 2023, J. Cosmology Astropart. Phys. **2023**(10), 044
- Beisbart, C. and Kerscher, M.: 2000, ApJ **545**(1), 6
- Bernstein, G. M. and Cai, Y.-C.: 2011, MNRAS **416**(4), 3009
- Cadiou, C.: 2022, *FyeldGenerator*
- Cai, Y.-C., Bernstein, G., and Sheth, R. K.: 2011, MNRAS **412**(2), 995
- Carron, J. and Szapudi, I.: 2013, MNRAS **434**(4), 2961
- Chiang, C.-T., Wagner, C., Sánchez, A. G., Schmidt, F., and Komatsu, E.: 2015, J. Cosmology Astropart. Phys. **2015**(9), 028
- Cuesta-Lazaro, C., Paillas, E., Yuan, S., Cai, Y.-C., Nadathur, S., Percival, W. J., Beutler, F., et al.: 2024, MNRAS **531**(3), 3336
- DESI Collaboration, Aghamousa, A., Aguilar, J., Ahlen, S., Alam, S., Allen, L. E., Allende Prieto, C., et al.: 2016, *arXiv e-prints* p. arXiv:1611.00036
- Friedrich, O., Gruen, D., DeRose, J., Kirk, D., Krause, E., McClintock, T., Rykoff, E. S., et al.: 2018, Phys. Rev. D **98**(2), 023508
- Giblin, B., Heymans, C., Harnois-Déraps, J., Simpson, F., Dietrich, J. P., Van Waerbeke, L., and Amon, o.: 2018, MNRAS **480**(4), 5529
- Gruen, D., Friedrich, O., Amara, A., Bacon, D., Bonnett, C., Hartley, W., Jain, B., et al.: 2016, MNRAS **455**(3), 3367
- Gruen, D., Friedrich, O., Krause, E., DeRose, J., Cawthon, R., Davis, C., Elvin-Poole, J., et al.: 2018, Phys. Rev. D **98**(2), 023507
- Hamaus, N., Seljak, U., and Desjacques, V.: 2011, Phys. Rev. D **84**(8), 083509
- Kovetz, E. D., Viero, M. P., Lidz, A., Newburgh, L., Rahman, M., Switzer, E., Kamionkowski, M., et al.: 2017, *arXiv e-prints* p. arXiv:1709.09066
- Laureijs, R., Amiaux, J., Arduini, S., Auguères, J. L., Brinchmann, J., Cole, R., Cropper, M., et al.: 2011, *arXiv e-prints* p. arXiv:1110.3193
- Lee, J. and Pen, U.-L.: 2008, ApJ **686**(1), L1
- Lombriser, L., Simpson, F., and Mead, A.: 2015, Phys. Rev. Lett. **114**(25), 251101
- Martino, M. C. and Sheth, R. K.: 2009, MNRAS **394**(4), 2109
- Massara, E., Villaescusa-Navarro, F., Ho, S., Dalal, N., and Spergel, D. N.: 2021, Phys. Rev. Lett. **126**(1), 011301
- McDonald, P. and Seljak, U.: 2009, J. Cosmology Astropart. Phys. **2009**(10), 007
- Morawetz, J., Paillas, E., and Percival, W. J.: 2025, J. Cosmology Astropart. Phys. **2025**(1), 026
- Newburgh, L. B., Addison, G. E., Amiri, M., Bandura, K., Bond, J. R., Connor, L., Cliche, J.-F., et al.: 2014, in L. M. Stepp, R. Gilmozzi, and H. J. Hall (eds.), *Ground-based and Airborne Telescopes V*, Vol. 9145 of *Society of Photo-Optical Instrumentation Engineers (SPIE) Conference Series*, p. 91454V
- Neyrinck, M. C. and Szapudi, I.: 2007, MNRAS **375**(1), L51
- Neyrinck, M. C., Szapudi, I., McCullagh, N., Szalay, A. S., Falck, B., and Wang, J.: 2018, MNRAS **478**(2), 2495
- Neyrinck, M. C., Szapudi, I., and Szalay, A. S.: 2009, ApJ **698**(2), L90
- Nikakhtar, F., Sheth, R. K., Padmanabhan, N., Lévy, B., and Mohayaee, R.: 2024, Phys. Rev. D **109**(12), 123512
- Paillas, E., Cai, Y.-C., Padilla, N., and Sánchez, A. G.: 2021, MNRAS **505**(4), 5731
- Paillas, E., Cuesta-Lazaro, C., Zarrouk, P., Cai, Y.-C., Percival, W. J., Nadathur, S., Pinon, M., et al.: 2023, MNRAS **522**(1), 606
- Paranjape, A., Hahn, O., and Sheth, R. K.: 2018, MNRAS **476**(4), 5442
- Planck Collaboration, Aghanim, N., Akrami, Y., Ashdown, M., Aumont, J., Baccigalupi, C., Ballardini, M., et al.: 2020, A&A **641**, A6
- Repp, A. and Szapudi, I.: 2017, MNRAS **464**(1), L21
- Repp, A. and Szapudi, I.: 2021, MNRAS **500**(3), 3631
- Repp, A. and Szapudi, I.: 2022, MNRAS **509**(1), 586
- Sheth, R. K.: 1998, MNRAS **300**(4), 1057
- Shi, J. and Sheth, R. K.: 2018, MNRAS **473**(2), 2486
- Simpson, F., Blake, C., Peacock, J. A., Baldry, I. K., Bland-Hawthorn, J., Heavens, A. F., Heymans, C., et al.: 2016, Phys. Rev. D **93**(2), 023525
- Simpson, F., Heavens, A. F., and Heymans, C.: 2013, Phys. Rev. D **88**(8), 083510
- Simpson, F., James, J. B., Heavens, A. F., and Heymans, C.: 2011, Phys. Rev. Lett. **107**(27), 271301
- Skibba, R., Sheth, R. K., Connolly, A. J., and Scranton, R.: 2006, MNRAS **369**(1), 68
- Szapudi, I., Branchini, E., Frenk, C. S., Maddox, S., and Saunders, W.: 2000, MNRAS **318**(4), L45
- White, M.: 2016, J. Cosmology Astropart. Phys. **2016**(11), 057
- White, M. and Padmanabhan, N.: 2009, MNRAS **395**(4), 2381
- Wolk, M., Carron, J., and Szapudi, I.: 2015, MNRAS **454**(1), 560
- Xu, T., Cai, Y.-C., Chen, Y., Neyrinck, M., Gao, L., and Wang, Q.: 2025, ApJ **982**(1), 5

APPENDIX A: BINNING DETAILS

In binning the values of $\hat{\xi}_I$ (for determining the green points in Fig. 1), there are cases in which we want every $\hat{\xi}_I$ -value to have its own bin (the most extreme of these cases being the extreme densities for which $\hat{\xi}_I$ is either undefined or -1 in any given realization). At the same time, if we have too many bins, shot noise will mimic true $\partial\mathcal{P}(\xi_I)/\partial A_z$.

Thus we use the following binning algorithm: suppose we have N_r realizations. Since $\hat{\xi}_I$ can be undefined, we will have N_r^{def} instances of defined $\hat{\xi}_I$ -values and $N_r - N_r^{\text{def}}$ cases in which it is undefined. Let n be the number of unique numerical (defined) values of $\hat{\xi}_I$ in this set. We begin with the lower of the two values $\sqrt{N_r^{\text{def}}}$ and n , and split the range of $\hat{\xi}_I$ into that many bins; this is our minimum number of bins. If all of these bins are full, we stop; if some of these bins are empty, we double the number of bins until either we have $\sqrt{N_r^{\text{def}}}$ full bins, or each unique value occupies its own bin. We treat cases in which $\hat{\xi}_I$ is undefined as occupying their own non-numerical bin, as when deriving Equation 41.

This procedure effectively errs on the side of having too many bins, thus leaving us open to shot noise masquerading as information. We attempt to correct for this pseudo-information as follows.

Consider the i th bin B_i . Since we perform the N_r realizations twice (for slightly different values of σ^2), we let N_{i1} , N_{i2} be the number of times (out of the first and second set of N_r realizations) that $\hat{\xi}_I$ falls into the bin B_i . Then the contribution of that bin to the total calculated information

is

$$\frac{(\mathcal{P}(B_i))'}{\mathcal{P}(B_i)} = \frac{2}{N_r(\Delta A_z)^2} \cdot \frac{(N_{i2} - N_{i1})^2}{N_{i1} + N_{i2}}, \quad (\text{A1})$$

letting $N_{i1} + N_{i2} = 2\mathcal{P}(B_i) \cdot N_r$. Let us assume that the only difference between N_{i1} and N_{i2} consists of random fluctuations, so that $\langle N_{i1} \rangle = \langle N_{i2} \rangle \equiv \bar{N}_i$. Then if we assume a binomial distribution for N_1, N_2 , we can write

$$\sigma_{N_i}^2 = \bar{N}_i \left(1 - \frac{\bar{N}_i}{N_r}\right). \quad (\text{A2})$$

Then, again approximating $N_{i1} + N_{i2} = 2\bar{N}_i$, we can say that the expected size of the fluctuations of $D_i \equiv (N_{i2} - N_{i1})^2 / (N_{i1} + N_{i2})$ is

$$\sigma_{D_i}^2 = \left(2 \langle (\Delta N_i)^2 \rangle + \frac{\langle (\Delta N_i)^4 \rangle}{8\bar{N}_i^2}\right) \left(\frac{1}{\bar{N}_i} - \frac{1}{N_r}\right), \quad (\text{A3})$$

where $\Delta N_i \equiv N_{i2} - N_{i1}$.

Since $N_{i1}, N_{i2} \sim \text{Bin}(N_r, \bar{N}_i/N_r)$, we can write

$$\langle (\Delta N_i)^2 \rangle = 2\sigma_{N_i}^2 = 2\bar{N}_i \left(1 - \frac{\bar{N}_i}{N_r}\right), \quad (\text{A4})$$

and

$$\begin{aligned} \langle (\Delta N_i)^4 \rangle &= 2\bar{N}_i \left(1 - \frac{\bar{N}_i}{N_r}\right) \\ &\quad \times \left[1 + 6\bar{N}_i \left(1 - \frac{\bar{N}_i}{N_r}\right) \left(1 - \frac{1}{N_r}\right)\right] \end{aligned} \quad (\text{A5})$$

$$\approx 2\bar{N}_i \left(1 - \frac{\bar{N}_i}{N_r}\right) \left[1 + 6\bar{N}_i \left(1 - \frac{\bar{N}_i}{N_r}\right)\right], \quad (\text{A6})$$

whence

$$\sigma_{D_i}^2 = q_i^2 \left(4 + \frac{1}{4\bar{N}_i^2} + \frac{3q_i}{2\bar{N}_i}\right), \quad (\text{A7})$$

where $q_i \equiv (1 - \bar{N}_i/N_r)$. It follows that the correction C for shot noise should be the sum in quadrature of these bin fluctuations, multiplied by the prefactor from Equation A1:

$$C^2 = \left(\frac{2}{N_r(\Delta A_z)^2}\right)^2 \sum_i q_i^2 \left(4 + \frac{1}{4\bar{N}_i^2} + \frac{3q_i}{2\bar{N}_i}\right), \quad (\text{A8})$$

where the sum is taken over all non-empty bins. It is this correction C which we use when calculating the green points in Fig. 1.

This paper has been typeset from a $\text{\TeX}/\text{\LaTeX}$ file prepared by the author.